Ionics (2009) 15:11–17
DOI 10.1007/s11581-008-0287-z

ORIGINAL PAPER

Preparation and characterization of $Li_2CoMn_3O_8$ thin film cathodes for high energy lithium batteries

Y. Bai · C. Knittlmayer · S. Gledhill · I. Lauermann · Ch.-H. Fischer · W. Weppner

Received: 23 March 2008 / Revised: 12 October 2008 / Accepted: 12 October 2008 / Published online: 15 November 2008

Abstract An ion layer gas reaction (ILGAR) dip-coating process for the deposition of homogeneous spinel structured $Li_2CoMn_3O_8$ thin layers has been developed. Thin film cathodes for use in high-energy density lithium batteries with thicknesses of about 200 nm have been prepared. The films were found to be X-ray amorphous after preparation. After annealing at 700°C in air for 2 h, the spinel structure of $Li_2CoMn_3O_8$ was observed by X-ray diffraction analysis. The composition of the surface was studied by XPS, which indicated enhanced Li and Mn concentrations as a result of the rinsing process and different solubilities of the precursor salts. The electrochemical behavior was investigated by separating the annealed electrode sample from a conventional organic lithium ion-conducting electrolyte by a layer of LiPON solid electrolyte and using elemental lithium as counter electrode. A capacity of 110.8 mAh/g was observed which is related to the valence changes of Mn and Co in the spinel structure.

Keywords Thin film battery · $Li_2CoMn_3O_8$ thin layers · ILGAR

Y. Bai · C. Knittlmayer · W. Weppner (✉)
Chair for Sensors and Solid State Ionics, Faculty of Engineering,
Christian-Albrechts-University,
Kaiserstr.2,
D-24143 Kiel, Germany
e-mail: ww@tf.uni-kiel.de

Y. Bai · S. Gledhill · I. Lauermann · Ch.-H. Fischer
Hahn-Meitner-Institute, SE 2,
Glienickerstr. 100,
D-14109 Berlin, Germany

Introduction

Rechargeable all-solid-state lithium batteries allow high-density energy storage with high chemical and electrochemical stabilities in combination with several solid electrolytes. Cathode materials with voltages more than 4 V vs. elemental lithium are applicable but cannot be used in combination with common liquid organic electrolytes [1–3]. Furthermore, stacks of thin films allow the formation of large electrolyte/electrode interfaces for batteries with high-power density. These films can be deposited directly onto electronic chips or chip packages of any shape or size, and flexible batteries can be made by printing onto plastics, thin metal foil or even paper [4].

For high-energy density batteries, different cathode materials have been investigated. Most of them are related to spinel-structured lithium manganese oxides with the general formula $Li_2Me_xMn_{4-x}O_8$ (Me = Co, Ni, Fe, Cr, or Cu) [5–17]. In this family of materials, the cobalt member with the stoichiometric formula $Li_2CoMn_3O_8$ shows presently the best performance [12] in view of reversible lithium intercalation. De-intercalation of lithium from spinel-structured lithium manganese oxides starts at a voltage of approximately 4 V. This voltage corresponds to the Gibbs energy of oxidation of Mn^{3+} to Mn^{4+}. In case of the presence of Co, a second voltage of approximately 4.8 V is observed due to the oxidation of Co^{3+} to Co^{4+}. For $Li_2CoMn_3O_8$, a specific capacity of 130 $mAhg^{-1}$ has been reported [12].

The present article reports a new preparation method for spinel-structured high-energy density cathode layers for lithium thin film batteries by the ion layer gas reaction (ILGAR) process. This is a low-cost thin-layer deposition technique which so far has successfully been used in the field of photovoltaics. The process allows preparation of homogeneous films on flat or rough substrates of any shape [20].

ILGAR technique

The ion layer gas reaction method was initially developed for the deposition of thin metal sulfide layers and was later extended to metal oxides. Both ILGAR sulfide and oxide layers are successfully used in chalcopyrite thin film solar cells resulting in excellent cell efficiencies. [18–21]. The cyclic ILGAR process [22–24] combines a wet-chemical coating with a solid–gas reaction. In a first step, a solid film of a metal precursor salt ("ion layer") is deposited by dipping the substrate into a metal salt solution. Secondly, the dry and solid precursor layer is chemically converted to the corresponding hydroxides by exposure to the reaction gas ("gas reaction"). The hydroxides undergo dehydration to the desired oxide according to the following equations:

$$M^{x+} + x\mathrm{H_2O_{gas}} + x\mathrm{NH_{3\,gas}} \rightarrow M(\mathrm{OH})_{x\ \mathrm{solid}} + x\mathrm{NH_4^+},$$
$$2M(\mathrm{OH})_x \rightarrow xM_{2/x}\mathrm{O} + x\mathrm{H_2O}$$
$$\left(M^{x+} = \mathrm{Li^+}, \mathrm{Mn^{2+}}, \mathrm{Co^{2+}}\right)$$

Thirdly, the as-prepared layer is dipped into a rinsing solution for removing by-products (e.g., NH_4Cl in case of chlorides) and unconverted reactants. Steps 1–3 are repeated cyclically until the desired thickness is reached. Between steps 1 and 2, a cooling and drying step by an inert gas stream can be added if necessary. This process is shown schematically in Fig. 1 and has been automated by an *x–y–z* robot. Since the growth rate per cycle is constant, the film thickness can be easily controlled and reproduced. Recently, the precursor solution has been also applied by spraying, which allows also large area and tape coating [25].

Experimental

For the investigation of $Li_2CoMn_3O_8$ prepared by ILGAR, three different types of substrates were used: quartz substrates for XRD measurements (XRD 3003, Seifert, Ahrensburg), Pt-coated Al_2O_3 (2.54 cm × 2.54 cm) for the gravimetric determination of the deposition rate and Au-coated Al_2O_3 for the electrochemical investigations (3.5 cm × 3.5 cm). All substrates were cleaned with isopropanol in an ultrasonic bath before deposition.

The precursor solution consisted of 10 mmol (1.61 g) $MnCl_2{\cdot}2H_2O$ (Merck), 2.75 mmol (1.02 g) $Co(ClO_4){\cdot}6H_2O$, and 25 mmol (1.06 g) LiCl (Merck) dissolved in a mixture of 125 ml ethanol (99.9% Sigma-Aldrich) and 125 ml distilled water. The dissolution was enhanced in an ultrasonic bath. A clean substrate was first dipped into the precursor solution, then moved to the oven for the gas reaction. The gas reaction phase for each cycle took place at 200°C in a stream of ammonia and water vapor, obtained by bubbling nitrogen through an aqueous ammonia solution for 60 s. Afterwards, the sample was rinsed in a 100-mM solution of LiOH (Merck) in ethanol (99.9% Sigma-Aldrich) to remove adsorbed ammonium chloride and perchlorate, respectively, as well as to prevent Li depletion. In some experiments, the surfactant "Triton X-100" (concentrate, Sigma-Aldrich) was added to the precursor solution (7.5×10^{-4} M) to study its effect on the surface morphology.

For XPS measurements, an Al K_α source and a CLAM4 electron spectrometer (Thermo VG Scientific) were used in the CISSY-UHV-facility.

For electrochemical investigation, a computer-controlled galvanostat/potentiostat (PG 1.0, Ionic Systems, Stuttgart) was used in galvanostatic mode. All investigations were carried out employing samples, which were deposited on Au thin films with a film thickness of about 200 nm. The samples were annealed after preparation at 700°C in air for 2 h. To avoid the direct contact between the liquid electrolyte and the $Li_2CoMn_3O_8$ film, a thin solid electrolyte LiPON layer was sputtered on top of the cathode [3]. The electrochemical measurements were performed in an

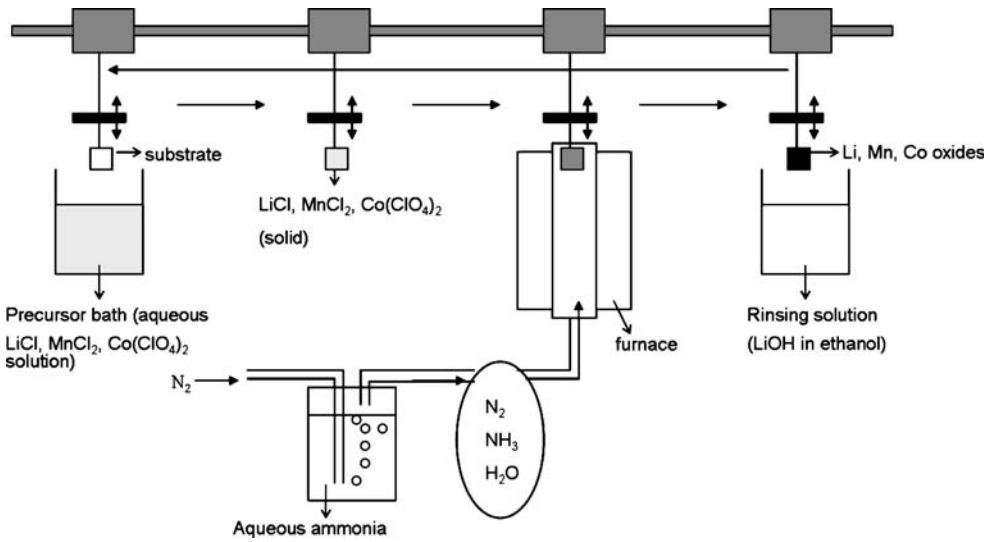

Fig. 1 Schematic illustration of the dip-ILGAR process

argon gas-filled glove-box. Interactions with traces of oxidizing or reducing gases were avoided by encapsulation of the galvanic cell. The sample was housed in a stainless steel container. A microporous membrane soaked-in with commercial electrolyte "Merck ZV 1352" was placed on top of the sample. A small sheet of lithium foil was applied as counter electrode. After assembling, the cell was closed with a Teflon cap. The cell arrangement was loaded for better electrical contact by a stainless steel cover. Electrical leads to the sample were made by a spring-loaded gold pin through a small hole in the cap.

Results

The thin films obtained with the ILGAR method were characterized with regard to the deposition rate, crystal structure, surface morphology, and electrochemical behavior.

Deposition rate In order to find the optimum deposition temperature, the deposition rate of the films was determined gravimetrically. Since the molar mass of $Li_2Mn_3CoO_8$ is quite high and the thickness of the film can reach 250–300 nm (30 dipping cycles), an analytical balance is sufficient to obtain an accurate growth rate of the films. For this purpose, samples were prepared on Pt thin films at reaction temperatures of 100, 200, 275°C for 60 s per cycle using the precursor solution without adding a wetting agent. After every fifth cycle, the mass of the samples was measured. The results are shown in Fig. 2. From the slopes of the fitted lines, the deposition rates were calculated (Table 1). The fact that the curves do not go through the zero point might be due to errors in the tare weights. However, this does not cause a problem, since the slopes of the curves are not affected. The entire deposition process took about 90min.

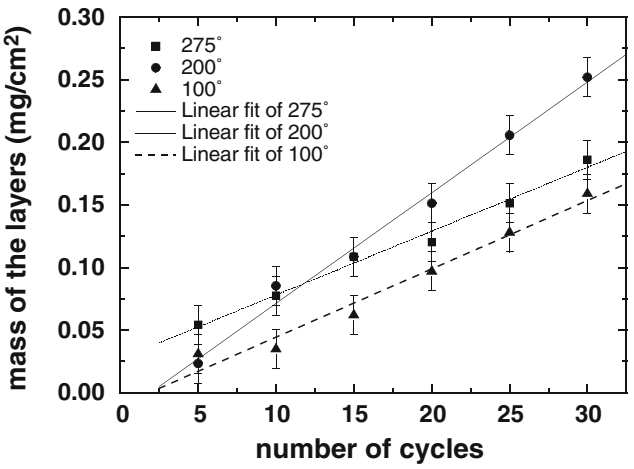

Fig. 2 Gravimetrically determined deposition rates of $Li_2CoMn_3O_8$ at different deposition temperatures (100, 200, and 275 °C). Substrate: Pt sputtered onto Al_2O_3

Table 1 Gravimetrically determined deposition rates of $Li_2Mn_3CoO_8$ films prepared by ILGAR on Pt thin films (2.54 cm × 2.54 cm)

Temperature T (°C)	Depostion rate, mg/(cm^2 cycle)
100	$5.4\times10^{-3}\pm7.4\times10^{-4}$
200	$8.8\times10^{-3}\pm7.4\times10^{-4}$
275	$5.1\times10^{-3}\pm7.4\times10^{-4}$

Crystal structure The XRD patterns of two different samples were taken in grazing incidence mode. All samples were prepared during 20 cycles on quartz substrates. The results are shown in Fig. 3. The first sample (a) was prepared at a reaction temperature of 200°C for 60 s, each cycle using the precursor solution without wetting agent. The XRD shows an X-ray amorphous behavior. After annealing in air at 700°C for 2 h, an XRD pattern was observed (b), which could be assigned to the cubic spinel phase of $Li_2CoMn_3O_8$ according to JCPDS 48 261. The second sample (c) was prepared in the same way as sample (a), but using a precursor solution with the addition of the wetting agent "Triton X-100" (7.5×10^{-4}M). This sample was annealed in air at 700°C for 2 h immediately after preparation. The composition is less pure than sample c.

Morphology Sometimes, horizontal stripes were observed on the sample surfaces. To improve homogeneity, two

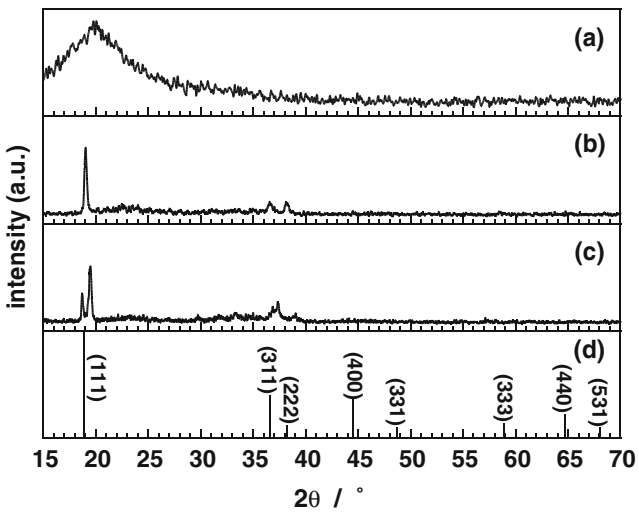

Fig. 3 XRD patterns of the deposited layers on quartz substrates: **a** sample prepared without wetting agent at 200 °C (as prepared), **b** sample prepared without wetting agent at 200 °C (annealed at 700 °C), **c** sample prepared with wetting agent Triton X-100 ($C=5\times10^{-4}$ mol/l) at 200 °C (annealed at 700 °C), **d** pattern of JCPDS card No 48: 261 for $Li_2CoMn_3O_8$

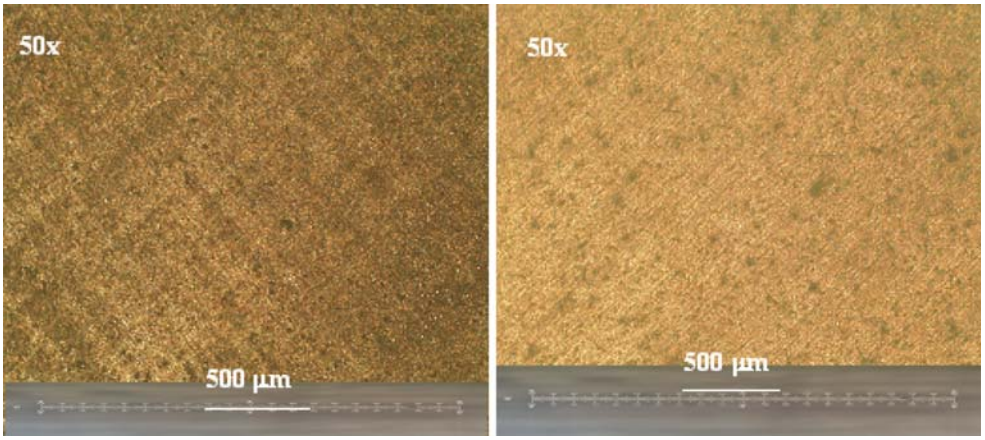

Fig. 4 Light microscope images of ILGAR $Li_2CoMn_3O_8$. *Left*: Sample prepared without wetting agent. *Right*: Sample prepared with wetting agent

approaches were used, both using standard deposition conditions on polished Al_2O_3 substrates at a reaction temperature of 200°C. The surface morphology was first investigated with a light microscope (Fig. 4). In the first approach, a sample, processed using the standard precursor solution, was rotated rotated by 90° five times during preparation (Fig. 4, left). An alternative approach to improve homogeneity was to improve the wetting properties of the aqueous/alcoholic solution. For this purpose, the wetting agent "Triton X-100" ($c = 7.5 \times 10^{-4}$M) was added to the precursor solution. The light microscope image of the resulting film is shown in Fig. 4, right.

SEM pictures were taken for investigating the microstructure (Fig. 5). For that purpose samples were prepared on Pt plates without wetting agent for 20 cycles at a reaction temperature of 200°C. After annealing in air at 700°C for 2 h, the sample shows an agglomerated structure.

The SEM cross-sections of these samples are shown in Fig. 6. The thicknesses of the films are in the range of 200 nm after annealing.

Surface Composition The surface compositions were analyzed with XPS. The samples were prepared by 20 cycles at a reaction temperature of 200°C on Pt plates. For comparison, a powder sample was prepared according to [2]. The overview spectra are shown in Fig. 7. The XPS signals of the elements Li, Co, Mn, and oxygen were found for all samples. From the peak areas, the elemental ratio of Li:Co:Mn at the surface was calculated to be

before annealing: Li:Co:Mn = 28: 1.3: 1,
after annealing: Li:Co:Mn = 57: 1: 3.4.

Besides the XPS signals of the elements of the spinel, the peaks of some impurities such as Na, Cl, C, N, and Mo were observed.

Electrochemistry Immediately after assembling the cell encapsulated into a stainless steel container with a teflon cover, as shown in Fig. 8, a potential of about 3.75 V was observed. During charging, a constant current of $I = 200\mu A$ was applied. The charging curve of the first cycle is shown in Fig. 9. The period from 1,000 to about 4,700 s is related to the valence change of manganese. During this process, Mn^{III} is oxidized to Mn^{IV}. This resulted in a final potential of about 4.5 V. Subsequently, a voltage step can be seen from 4.5 to 4.8 V. This may be attributed to the starting valence change of cobalt. During this process, Co^{III} is oxidized to Co^{IV}. After 6,700 s, the oxidation of Co^{III} is completed with a final voltage of 5 V. The specific capacity for the charging process is C=110.8 mAh/g.

After the charging process, the reverse current of $I = -200\ \mu A$ was applied, and the battery was discharged.

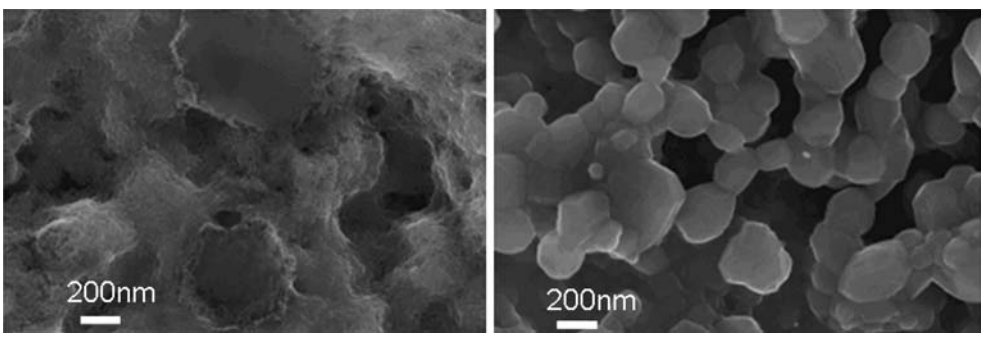

Fig. 5 SEM top view images of $Li_2CoMn_3O_8$ samples prepared at 200 °C using the precursor solution without adding wetting agent Triton X-100. *Left*: As-prepared; *Right*: Annealed for 2 h in air at 700 °C

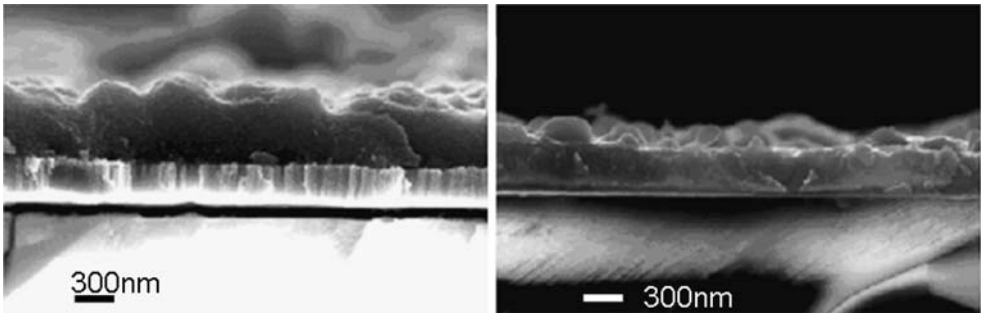

Fig. 6 SEM cross-section images of $Li_2CoMn_3O_8$ samples prepared at 200° using the precursor solution without wetting agent Triton X-100. *Left*: As-prepared; *Right*: Annealed for 2 h in air at 700 °C

Instantaneously, a large IR drop from 5 to 3.3 V was observed. It is obvious that the discharging process is much shorter than the charging process, and the starting as well as the final electrostatic potentials are lower than in the case of charging.

From the charge transport for the two oxidation processes, atomic Mn to Co ratios in the cathode were calculated to be Mn:Co=2.0:1 for the charging process and Mn:Co=2.3:1 for the discharging process.

Discussion

$Li_2CoMn_3O_8$ thin films could be prepared by ILGAR. The surface composition was measured by XPS. Ratios of Li:Co:Mn=28:1.3:1 for the as-prepared sample and Li:Co:Mn=57:1:3.4 for the crystalline sample were calculated. The measured high excess of lithium can be explained by the fact that the samples were rinsed in a lithium hydroxide-containing solution during the last process step. Thus, lithium is highly concentrated in the surface layer and does not reflect the bulk composition.

The measured difference in the ratio of Co:Mn can be explained by the different solubility of $MnCl_2$ and $Co(ClO_4)_2$ in the precursor solution. During the evaporation of the solvents from the liquid precursor film, at first, the less soluble $MnCl_2$ is precipitating on the substrate, followed by the better soluble $Co(ClO_4)_2$. Thus, a layered microstructure of a manganese layer with a cobalt-rich layer on top is obtained. During annealing, the elements of these microlayers interdiffuse, so that a homogeneous distribution of cobalt and manganese ions is obtained within the film after crystallization.

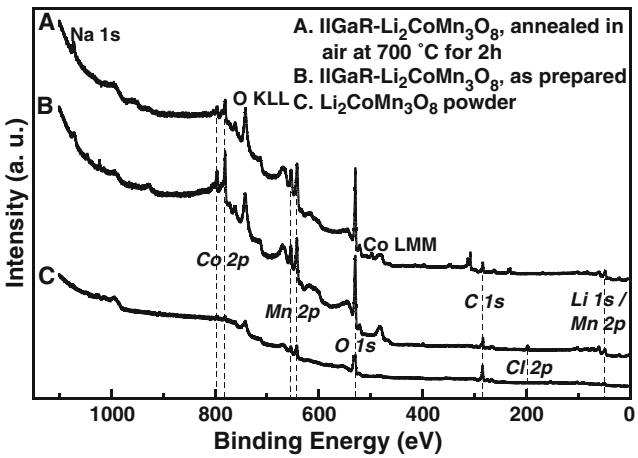

Fig. 7 XP spectra of $Li_2CoMn_3O_8$ prepared by ILGAR, as deposited (**b**), after annealing (**a**) as well as powder preparation (**c**)

The Co^{3+}:Mn^{3+} ratios of 1:1.9 and 1:2.3 determined from the electrochemical measurements for charging and discharging, respectively, take into account that only Mn^{3+} and Co^{3+} ions are present. However, both Mn and Co have a formal valence of 3.5 in the spinel structure ($A_2B_4O_8$) of $Li_2CoMn_3O_8$ since both are placed on the B-site in $A_2B_4O_8$, i.e., B^{3+} and B^{4+} are contained in $A_2B_4O_8$ in a ratio of 1:1. Since Mn^{4+} is slightly more stable than Co^{4+}, it is favorable that $Li_2CoMn_3O_8$ contains more Mn^{4+} than Co^{4+}. Thus, the measured Co^{3+}:Mn^{3+} ratio is slightly shifted to a higher content of Co than that measured by XPS.

The two alternatives for improving the homogeneity were constructive. Often, structural stripes at the surface of the layers were observed. One reason may be small waves in the bath generated by moving the sample or insufficient wetting of the aqueous-alcoholic solution. When the sample was turned around by 90° several times during the process, the microscopic image still showed stripes, but now crossing under an angle of 90° and were much less pronounced than without rotating The addition of the wetting agent Triton X-100 improved the homogeneity without turning the sample. Thus, this allows more homogeneous coatings of other materials with aqueous solvents using the Dip-ILGAR process.

The charging curve of the galvanic cell

$$Pt|Li_2CoMn_3O_8|LiPON|electrolyte(liq.)|Li$$

shows two voltage plateaus at cell voltages of 3.8–4.1 and 4.8–5.0 V. The lower one could be assigned to the oxidation of Mn^{3+} to Mn^{4+}, the higher one to the oxidation of Co^{3+} to Co^{4+}. The specific capacity was calculated from the charging time to be C=110.8 mAh/g. This value matches the specific capacity given in the literature [12] within the limit of error.

The large voltage drops observed upon changing the direction of the current may be attributed to a high inner

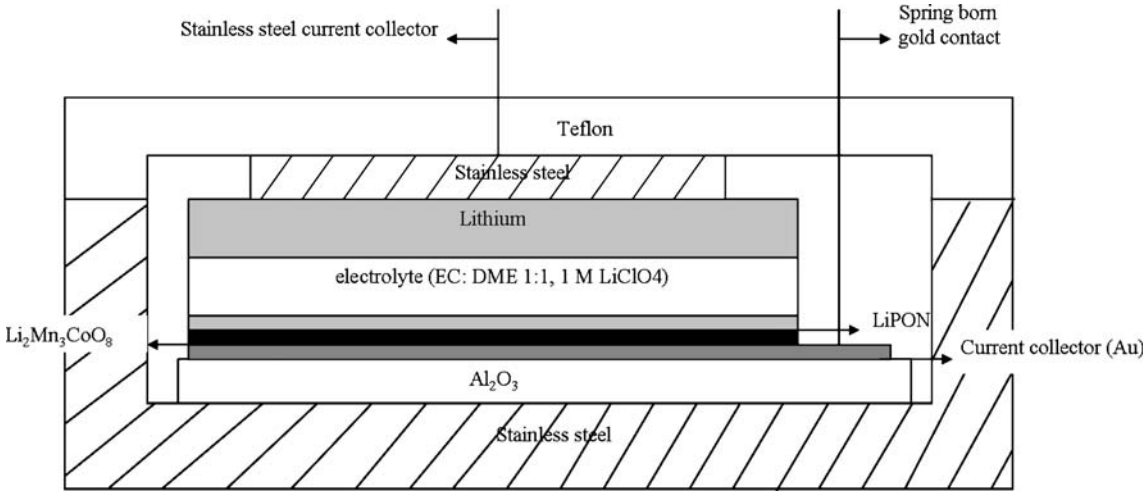

Fig. 8 Schematic representation of the galvanic cell arrangement for electrochemical measurements

cell resistance and to the polarization of the interfaces between the electrolyte and the electrodes. The bulk resistance of the thin LiPON layer should only contribute a few millivolts to the voltage drop. It is likely that the organic electrolyte has been partially decomposed due to the high voltages applied during charging, which may have produced almost nonconducting layers at the interfaces between the electrodes and the electrolyte. Furthermore, the low diffusion coefficient of lithium intercalation in Li_x-$CoMn_3O_8$ may have rapidly polarized this electrode of the galvanic cell. This polarization of $Li_xCoMn_3O_8$ may be also one reason for the observed lower capacity of the cell upon discharge compared to the charging process.

Another reason for the lower discharging than charging capacity may be the partial loss of oxygen of the $Li_xCoMn_3O_8$ electrode, which is a result of the increasing oxygen activity at the very low lithium activity when the cell is charged at high voltages according to the Duhem–Margules relationship.

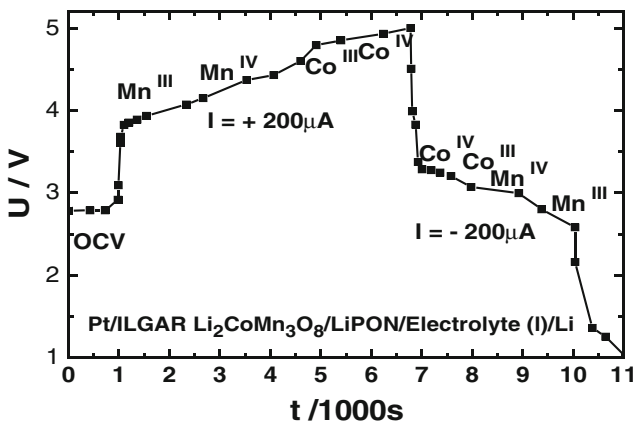

Fig. 9 Charging and discharging voltages of ILGAR prepared $Li_2CoMn_3O_8$ vs. elemental lithium as a function of time upon applying a constant electrical current of 200 μA

As a consequence, the valence of manganese and cobalt will change independently of the uptake or loss of lithium.

Finally, it should be taken into account that the amount of organic electrolyte is large compared to the amount of $Li_2CoMn_3O_8$. With a density of 4.8 g/cm^3 of the sample, the mass ratio of active electrode material to electrolyte, $M_{Li2CoMn3O8}$:$M_{electrolyte}$, is about 3×10^{-6}. This means that a small variation in the stoichiometry of the electrolyte in the range of 10^{-4}% corresponds to a change of x=0.12 for x in $Li_xCoMn_3O_8$ or a loss in specific capacity of 0.1%.

Conclusions

A new method for the preparation of $Li_2CoMn_3O_8$ thin films for use in high-energy density lithium batteries has been developed. This ILGAR technique is fast, simple, and has low cost. It is the first time that a quaternary compound has been deposited successfully by this technique. Two alternatives, turning of the sample during the process and addition of wetting agents, improve the layer homogeneity in the case of poorly wetting aqueous precursor solutions. Instead of dipping, also spraying can be used for the application of the precursor solution [22], which is even more favorable for industrial processes.

The obtained films show an X-ray amorphous microporous structure after deposition. After annealing at 700 °C in air for 2 h, the desired spinel structure was observed. In an electrochemical cell set-up, the charging and discharging performance was analyzed. The specific capacity was C= 110.8 mAh /g upon charging.

The ILGAR technique is capable to produce cathode films for liquid electrolyte and all-solid-state lithium batteries. It seems reasonable to assume that also layers of the other components of such batteries can be produced by the ILGAR technique.

References

1. Julien C, Ybka B, Guesdon JP (1995) Ionics 1:316
2. Schwenzel J (2003) Entwicklung und Charakterisierung von Dünnschicht-Akkumulatoren auf Basis von Festkörpermaterialien, Doctoral Thesis, Faculty of Engineering, Christian-Albrechts-University, Kiel, Germany
3. Weppner W, Schwenzel J (2003) Ionics 9:348
4. Lee SH, Liu P, Tracy CE, Benson DK (1999) Electrochem and Sol State Lett 2:425
5. Fey GTK, Li W, Dahn JR (1994) J Electrochem Soc 141:2279
6. Ohzuku T, Kitagawa M, Hirai T (1990) J Electrochem Soc 137:769
7. Sigala C, Guyomard D, Verbaere A, Piffart Y, Tounoux M (1995) Solid State Ionics 81:167
8. Amine K, Tukamoto H, Yasuda H, Fujita Y (1997) J Power Sources 68:604
9. Zhong Q, Bonakdarpour A, Zhang M, Gao Y, Dahn JR (1997) J Electrochem Soc 144:205
10. Kawai H, Nagata M, Tukamoto H, West A (1998) J Mater Chem 8:837
11. Ein-Eli Y, Howard Jr WF, Lu SH, Mukerjee S, McBreen J, Vaughey JT, Thackeray M (1998) J Electrochem Soc 145:1238
12. Kawai H, Nagata M, Tukamoto H, West A (1999) J Power Sources 81/82:67
13. Wu XM, Li XH, Xu MF, Zhang YH, He ZQ, Wang Z (2002) Mater Res Bull 37:2345
14. Jiang J, Burmester T, Eberman KW, Krause LJ, Dahn JR (2005) J Electrochem Soc 152:A19
15. Molenda J, Palubiak D, Marzek J (2005) J Power Sources 144:176
16. Li J, He X, Fan M, Zhao R, Jiang C, Wan C (2006) Ionics 12:77
17. Amdouni N, Zaghib K, Gendron F, Mauger A, Julien CM (2006) Ionics 12:117
18. Fischer ChH, Muffler HJ, Lux-Steiner MCh (2002) German Patent DE 50 000 568T2
19. Fischer ChH, Lux-Steiner MCh, Möller J, Könenkamp R, Siebentritt S (2007) German Patent DE 59914444.0-08T2
20. Allsop NA, Schönmann A, Muffler HJ, Bär M, Lux-Steiner MC, Fischer ChH (2005) Prog Photovolt: Res Appl 13:607
21. Bär M, Muffler HJ, Fischer CH, Zweigart S, Karg F, Lux-Steiner MCh (2002) Prog Photovolt.: Res Appl 10:173
22. Bär M, Muffler HJ, Allsop N, Fischer CH (2005) Recent Res Devel Crystal Growth 4:211
23. Bär M, Fischer CH, Lux-Steiner MC (2001) Sol Energy Mater Sol Cells 113:67
24. Möller J, Fischer CH, Muffler HJ, Könenkamp R, Kaiser I, Kelch C, Lux-Steiner MCh (2000) Thin Solid Films 113:361
25. Allsop NA, Schönmann A, Belaidi A, Muffler HJ, Mertesacker B, Lux-Steiner MCh, Fischer ChH (2005) Thin-Film Compound Semiconductor Photovoltaics, edited by Shafarman W, Gessert T, Niki S, Siebentritt S (Mater Res Soc Symp Proc 865, Warrendale, PA), F14.23